第 34 卷第 4 期
2015 年 8 月

红 外 与 毫 米 波 学 报
J. Infrared Millim. Waves

Vol. 34, No. 4
August, 2015

文章编号: 1001 - 9014(2015)04 - 0406 - 05

DOI:10.11972/j.issn.1001 - 9014.2015.04.005

A wide-angle and polarization insensitive highly-tunable infrared metamaterial perfect absorber

HOU Jian-Zhang[1], GU De-En[1*], WANG Tao[1], WEN Qi-Ye[2], JIANG Ya-Dong[1]

(1. School of Optoelectronic In formation, University of Electronic Science and Technology of China, Chengdu 610054, China;
2. School of Microelectronics and Solid-State Electronics, University of Electronic Science and Technology of China, Chengdu 610054, China)

Abstract: A highly-tunable wide-angle metamaterial absorber with perfect absorption and polarization-insensitivity was introduced and investigated. Simulative results show the maximum absorption reaches up to 99.9% at 5.8 μm and the absorber can be tuned arbitrarily in the range of 3.4 μm to 8.6 μm with the absorption remaining above 95% by changing its geometric parameters. The absorber remains absorptivity of over 95% with incident angles below 80° under transverse magnetic(TM) polarization and that of over 92% below 60° under transverse electric(TE) polarization. Furthermore, the absorber is polarization insensitive with polarization angle varying from 0° to 90°.

Key words: metamaterial, absorber, infrared, tunable
PACS: 78.67.Pt, 78.20.Ci, 42.25.Bs

一种宽角度极化不敏感的高可调谐红外超材料完美吸波体

侯剑章[1], 顾德恩[1*], 王 涛[1], 文岐业[2], 蒋亚东[1]

(1. 电子科技大学 光电信息学院,四川 成都 610054;
2. 电子科技大学 微电子与固体电子学院,四川 成都 610054)

摘要:提出了一种高度可调、宽角度且具有完美吸收和极化不敏感的超材料吸波体.模拟的结果显示,在5.8μm处可达到最高吸收率99.9%;通过改变其几何参数,吸波体的谐振波长在3.4μm到8.6μm的范围内可任意地调节,且都具有不低于95%的峰值吸收率.在横磁波下,当入射角度小于80°时,吸波体的吸收率保持在95%以上;在横电波下,当入射角小于60°时,吸收率保持在92%以上.此外,极化角度在0到90°变化时,吸波体具有极化不敏感性.

关 键 词:超材料;吸波体;红外;可调谐

中图分类号:TN21 **文献标识码**:A

Introduction

In the past decade, enormous researches have been reported in the field of metamaterials. As artificial composite structures with sub-wavelength resonant element arrays[1], metamaterials exhibit many exotic applications[2-5]. The metamaterial absorber is one of prominent applications[6-7]. The absorbers with "perfect" absorption could be good candidates for many exotic applications including thermal bolometers[8], spectrally selective infrared thermal detectors[9] and sensors[10]. After the first experimental demonstration of perfect absorber in the microwave regime[11], different structures have been proposed across wide spectra from microwave to optical frequencies[12-16]. Of all, a patterned metal layer over ground plane separated by a dielectric layer is a typical resonant absorber with perfect absorption[14, 17-19].

Generally, the resonant absorption remarkably depends on the incident and polarization angles[19]. Designing a wide-angle and polarization insensitive perfect resonant absorber is important for many practical applica-

Received date: 2014 - 06 - 13, **revised date**: 2015 - 06 - 04 **收稿日期**:2014 - 06 - 13, **修回日期**:2014 - 06 - 04
Foundation items: Supported by National Natural Science Foundation fo China (62135006,61131005), the fundamental Researc Funds for the Central Universities (ZYGX2012J058), and Key Grant Project of Chinese Ministry of Education (313013)
Biography: HOU Jian-Zhang(1990-), male, Jinzhou, Hubei province, master. Research area involves the design and research of new functional materials. Email: houjianzhang@msn.com
* **Corresponding author**: E-mail: gudeen@163.com

tions. An electrically coupled ring resonator (ERR) with fourfold rotational symmetry combined with a cross has been realized for a polarization insensitive terahertz (THz) absorber[20]. Many structures with rotational symmetry have been used for polarization independent response at the microwave[12], THz[20-21] and infrared[10, 17]. Most of these symmetrical structures are also wide-angle absorbers[10, 21-24]. A perfect absorber at near-infrared consisting of a two-dimensional gold disk array and a gold mirror separated by a dielectric spacer can absorb light with the simulated absorptivity of above 96% for TM mode below 80° incidence, and above 90% for TE mode below 50° incidence[10].

Traditional infrared devices, such as micrbolometers, have been designed to absorb uniformly across wide spectral bands. However, the wavelength tunability could be crucial for other applications, for instance, target recognition, chemical detection and so on[9]. For these applications, it is highly desirable to realize wavelength-tunable to reduce cost and enable the design of multi-detector arrays responding to different wavelengths[25]. The metamaterial absorbers with high-tunability could be well-suited for these devices. Although the tunability of a metamaterial perfect absorber seems easy by changing the dimension of the basic structure[6], keeping perfect peak absorption of an absorber within the spectral range of interest is rarely reported. Thomas Maier et al. evaluated the tunability of the absorber designed for microbolometers[8]. The peak simulated absorption varies from 82% to 98% with the peak wavelength tuned from 2.9 μm to 5.4 μm.

In this paper, we presented a highly-tunable, wide-angle and polarization insensitive IR absorber based on metamaterial structure with the simulated absorptivity of 99.9% at resonance wavelength. The absorber is a typical metal-dielectric-metal structure consisting of a novel cross-ring resonator, a dielectric spacer and a metal ground layer. The absorber we proposed remains perfect absorption with the absorptivity of over 95% at the incident angles below 80° for TM polarization and over 92% below 60° for TE polarization. Especially, the absorption of the absorber is still perfect with the absorptivity of over 95% within the wide resonance wavelength range from 3.4 μm to 8.6 μm by changing the dimension of the top structure. This makes the absorber more advantageous in applicable devices.

1　The structure designs and simulations

The unit cell structure of the designed infrared absorber is shown in Fig. 1(a). It consists of three layers, a 0.1 μm gold cross-ring resonator and a 0.1 μm gold ground plane, which are separated by a continuous MgF_2 film with the thickness of 0.13 μm. The three layers are fabricated on silicon substrate. Its dimension parameters are as follows: $D_x = D_y = 2$ μm, $W = 0.15$ μm, $L = 1.8$ μm, $R = 0.4$ μm, $r = 0.3$ μm.

We calculated the absorption by $A(\omega) = 1\text{-}R(\omega)\text{-}T(\omega)$, where $R(\omega)$ and $T(\omega)$ are the reflectance and transmittance of absorber, respectively. We set the thickness of gold ground plane as 0.1 μm, which is greatly larger than the skin depth of gold[26]. Thus the $T(\omega)$ is zero across the entire wavelength range. The effective electric $[\varepsilon(\omega)]$ and

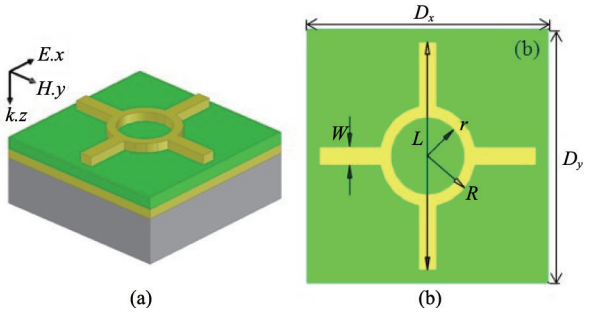

Fig. 1　(a) Schematic diagram of a single cell of the infrared absorber we designed and the incident EM waves polarization configuration. (b) Geometry of the top layer
图 1　(a)单个红外吸波体单元及入射电磁波方位示意图, (b)顶层几何结构图

magnetic response $[\mu(\omega)]$ of metamaterial structure can be tuned individually by changing the dimension and shape of metallic elements. So we can match the impedance $Z = [\mu(\omega/\varepsilon(\omega))]^{1/2}$ of the absorber to the free space through modulating the frequency and amplitude of the electric and magnetic response. So, the reflectance minimizes and the maximum absorption can be achieved at a specific frequency.

The dimension of the unit cell structure was defined in Fig. 1(b). The unit cells are periodically placed along x and y directions. The optimized structure of the absorber was achieved through numerical computations using COMSOL Multiphysics 4.3. We considered a sole unit cell with the EM waves incident along the z axis on the top layer, as shown in Fig. 1(a). The periodic boundary conditions are applied in y-z plane and x-z plane. Refractive index values of materials were taken from the sources[27-29]. The reflectance and transmittance dependence on frequency were obtained from the scattering parameters in the simulation package and the absorbance was calculated as $A(\omega) = 1\text{-}R(\omega)\text{-}T(\omega)$[30], where $R(\omega) = |S_{11}|^2$ and $= |S_{21}|^2$.

2　The results and discussion

The reflection, transmission and absorption spectra of the absorber, with the incident beam normal to the top layer of the structure and the electric field linearly polarized along the x axis, are shown in Fig. 2. is zero across the entire wavelength range, and the absorber can realize the absorption of 99.9% at 5.8 μm, which is near-perfect absorption. Furthermore, the width of the wavelength with the absorption greater than 90% is 0.23 μm. All these data we attained indicate the designed absorber is an excellent absorber.

In order to disclose the physical mechanism of perfect absorption in the designed absorber, we evaluated electromagnetic field, surface current distribution and the electromagnetic power loss at resonance wavelength under normally incident light.

The electric and magnetic field modulus of the cross-section parallel with x-z plane at $y = 1$ μm are shown in Fig. 3(a) and Fig. 3(b), respectively The near-unity absorption is attributed to both the electric and magnetic resonances. As the electric field of incident

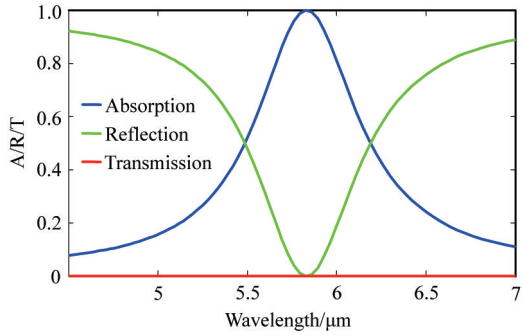

Fig. 2 The absorption (blue line), reflection (green line) and transmission (red line) spectra of the absorber
图2 吸波体的吸收曲线(蓝)、反射曲线(绿)和透射曲线(红)

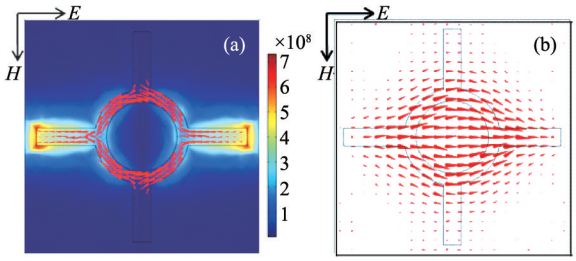

Fig. 4 (a) Distribution of electric field modulus (colormaps) and surface current (red arrows) on the undersurface of resonant element, and (b) distribution of surface current (red arrows) on the ground plane at resonance wavelength
图4 在谐振波长处,(a)谐振结构下表面的电场模(彩色图)和表面电流(红色箭头)分布;(b)底层表面的表面电流分布(红色箭头)

light drive, the gold cross-ring units at the top work as electric dipole resonators[30]. Obviously, the distribution of the electric field in Fig. 3(a) indicates the strong excitation of dipoles. There are strong electric field gathered at the gap of the two bars of adjacent cells [see in Fig. 3(a)] owing to strong electric field coupling. It also shows that the electric field is concentrated in the dielectric layer.

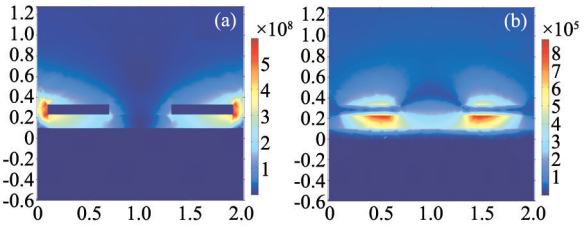

Fig. 3 The electric field modulus (a) and magnetic field modulus (b) distribution of the plane parallel with *x*-*z* plane at $y = 1$ μm
图3 在 $y = 1$ μm 处,平行于 *x*-*z* 平面处的电场模(a)和磁场模(b)分布

The electric field modulus and surface current distribution on the surface of resonant element are shown in Fig. 4(a), and Fig. 4(b) shows the surface currents distribution of ground plane. Strong electric dipole resonances in the top structure are caused by the charges accumulated at left side of bar, which leads to the surface current flow along the bar and ring from right to left. The direction of surface current of ground plane is opposite to the top layer. The anti-parallel currents in two metallic layers originating from the excitation of the magnetic field form circulating current loops[30]. The circulating current results in the accumulation of magnetic field in the dielectric layer as shown in Fig. 3(b). The localized magnetic field causes strong magnetic dipolar resonances[31], which also contributes to the absorption. Fig. 5 shows the electromagnetic power loss density of the cross-section parallel with *x*-*z* plane at $y = 0.5$, 0.8 and 1.0 μm. All these results reveal the energy loss mainly occurs in the two metallic layers and the ohmic loss is greater than the dielectric loss.

The designed absorber is perfectly angle-insensitive, as shown in Fig. 6(a) and (b). Considering that the incident waves parallel with the surface have no significance for practical application, the angular dispersion of the absorption spectra was investigated with the incident angles from 0° to 80°. Here, we set the the azimuthal angle as 0°. For the TE (the incident plane is parallel to *y*-*z* plane, and the electric field is fixed along the *x* direction) mode, the peak wavelength almost does not change from 0° to 80°. The peak absorption remains above 92% at the resonance wavelength for the incident angle up to 60°. The absorptivity decreases monotonically with the angle larger than 60°. This can be ascribed to tapering parallel magnetic field component.[14, 22, 32] For the TM (the incident plane is parallel to *x*-*z* plane, and

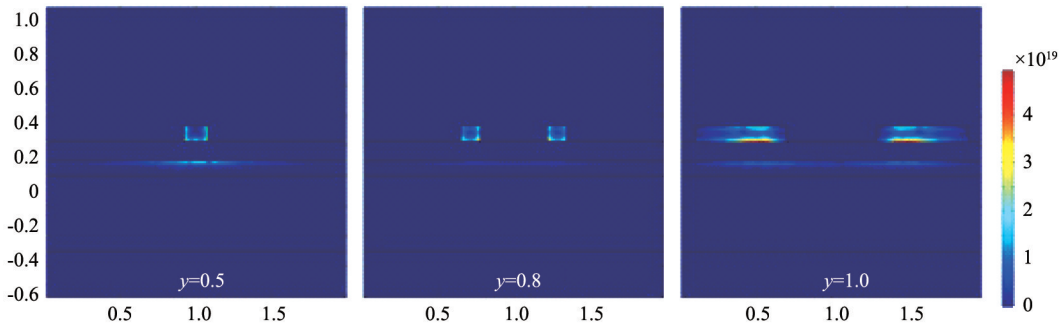

Fig. 5 The electromagnetic power loss density of the cross-section parallel with *x*-*z* plane at $y = 0.5$, 0.8 and 1.0 μm
图5 在 $y = 0.5$, 0.8 和 1.0 μm 处,平行于 *x*-*z* 平面的横截面处的电磁功率损耗密度

the magnetic field is fixed along the y direction) mode, the peak absorption remains above 95% for incident angle varying from 0° to 80°. It is because the magnetic field can still efficiently drive the circulating currents with the incident angle increasing[32]. Fig. 6(b) also shows the resonance wavelength has a little blue-shift with the angle greater than 40°, and the phenomenon of blue-shift we observed here is quite consistent with the reported results[23,31]. For normal incidence (or small incident angle), the dipole oscillation of cross-ring structure in every unit is in phase. Along the x direction, the existence of the attractive force between the positive and negative charges in the neighboring cross-ring weakens the restoring force of charge oscillation inside the cross-ring structure. With the incident angle increasing, the oscillation of electric dipole of neighboring cross-ring structure is no longer in phase, which results in the decrease of attractive force, thus the restoring force increases[33]. Therefore, the resonance frequency increases. The simulation results reveal that the designed absorber operates very well for a quite wide angle of incidence under both TE and TM modes. In practical application, such as spectrally selective infrared thermal detectors[9], it is critical for absorbers to absorb as much of the radiation as possible and be independent of the direction of incidence.

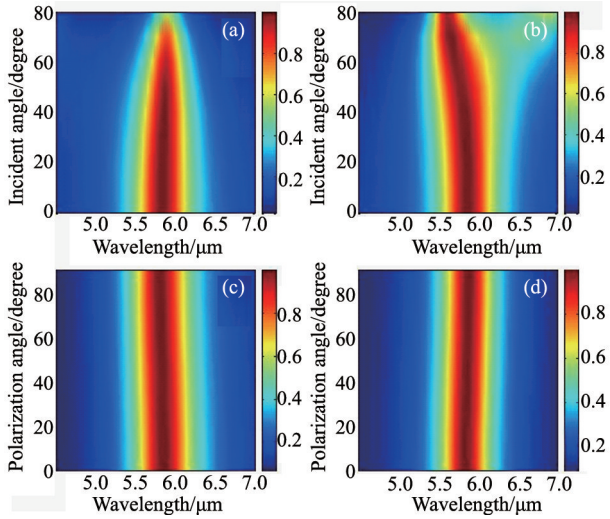

Fig. 6　The absorption as a function of incident angle and wavelength for TE (a) and TM (b) waves. The absorption as a function of both polarization angle and wavelength for TE (c) and TM (d) polarization

图 6　TE 波(a)和 TM 波(b)下的吸收率随入射角度和波长的变化;TE 极化(c)和 TM 极化(d)下的吸收率随极化角度和波长的变化

Polarization insensitive is another excellent feature of the proposed absorber, which is desirable in practical applications[8,14]. In order to demonstrate the polarization insensitivity of our absorber, the absorption spectra are shown in Fig. 6(c) for TE mode and in Fig. 6(d) for TM mode. Here, for both TE and TM, we set the incident plane pass through z axis, and the included angle between incident plane and y axis is the polarization angle. Considering that the absorber has perfect absorption with the incident angle from 0° to 60°, we set the incident angle as 30°. Fig. 6(c) and Fig. 6(d) indicate that the absorptivity and the full width half maximum (FWHM) are almost unchanged with polarization angle varying from 0° to 90° for both TE and TM modes. This reveals that the proposed absorber is nearly polarization insensitivity. This can be attributed to four-fold rotational symmetry of the designed unit cell[12, 14].

Most reported metamaterial perfect absorbers are confined to a fixed-frequency regime[17, 18, 22, 32]. However, a highly-tunable absorber is desirable for practical applications, such as spectrally selective infrared thermal detectors[9]. The metamaterial absorber we proposed can solve it perfectly. The tunability of the designed absorber was evaluated by changing the dimension of the top structure. Fig. 7(a) shows the absorption spectra of the absorber for the bar length L varying from 0.9 μm to 1.95 μm with W = 0.15 μm. The resonance wavelength increases from 3.4 μm to 7.1 μm. The peak absorptivity of all the absorbers with the incremental bar length keeps above 96%, and the relative FWHM (the ratio of FWHM to the resonance wavelength) increases a little from 10% to 12.7%. Similar results can be obtained by modulating the bar width W. As shown in Fig. 7(b), when W is modulated from 0.1 μm to 0.5 μm (L = 1.8 μm), the resonance wavelength increases from 5.6 μm to 6.7 μm. And the peak absorptivity of the absorbers is above 98% within the modulation range of W, the relative FWHM broadens slightly from 12% to 13.8%.

In addition, the effect of simultaneously varying L and W on the absorption of the absorber was investigated in Fig. 7(c). When the resonance wavelength is tuned from 3.4 μm to 8.6 μm by simultaneously increasing L and W, all the peak absorptivities still stay above 95%, and the relative FWHM broadens a little from 10.2% to 14.6%. All the above-mentioned results reveal that the absorber is highly tunable.

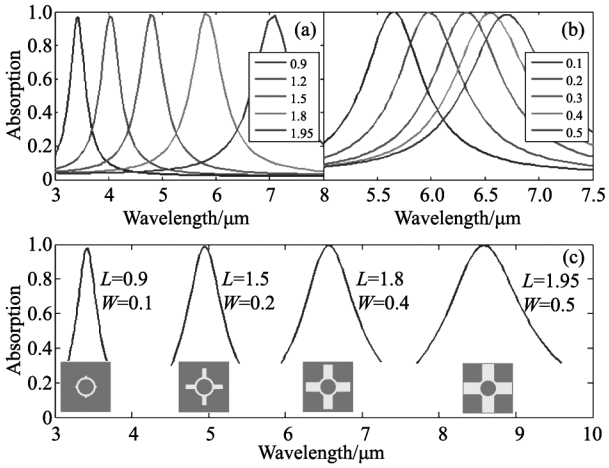

Fig. 7　(a) The absorption spectra for different L with W = 0.15 μm. (b) The absorption spectra for different W with L = 1.8 μm. (c) The absorption curve for different L and W

图 7　(a)当 W = 0.15 μm 时,不同 L 下的吸收曲线;(b)当 L = 1.8 μm 时,不同 W 下的吸收曲线;(c)不同 W 和 L 下的吸收曲线

3 Conclusions

In conclusion, we have designed and investigated a highly-tunable and wide-angle absorber based on metal-dielectric-metal metamaterial structure with the properties of perfect absorption and polarization-insensitivity in the infrared regime. It can achieve nearly unit absorption and remains high absorptivity even at large incident angles under TE and TM modes. We also demonstrated that the absorber is polarization insensitive. More importantly, the resonance wavelength can be manipulated in a wide wavelength range by changing the dimensions of the resonant element: the length and width of the bar. The structure of metamaterial absorber we proposed is very simple, and may have a bright prospect for improving the performance of the devices involving selective infrared absorption or emission.

Acknowledgements

This work is supported by the National Natural Science Foundation of China (Grant Nos. 62135006 and 61131005), the Fundamental Research Funds for the Central Universities (Grant No. ZYGX2012J058), and Key grant Project of Chinese Ministry of Education (Grant No. 313013).

References

[1] Ginn J, Shelton D, Krenz P, *et al.* Altering infrared metamaterial performance through metal resonance damping [J]. *J. Appl. Phys.*, 2009, **105**(7): 074304.
[2] Schurig D, Mock J J, Justice B J, *et al.* Metamaterial electromagnetic cloak at microwave frequencies [J]. *Science*, 2006, **314**(5801): 977-980.
[3] Pendry J B. Negative refraction makes a perfect lens [J]. *Phys. Rev. Lett.*, 2000, **85**(18): 3966-3969.
[4] Chen H T, O'Hara J F, Azad A K, *et al.* Experimental demonstration of frequency-agile terahertz metamaterials [J]. *Nat. Photonics*, 2008, **2**(5): 295-298.
[5] Ok J G, Seok Youn H, Kyu Kwak M, *et al.* Continuous and scalable fabrication of flexible metamaterial films via roll-to-roll nanoimprint process for broadband plasmonic infrared filters [J]. *Appl. Phys. Lett.*, 2012, **101**(22): 223102.
[6] Cheng Y Z, Yang H L, Cheng Z Z, *et al.* Perfect metamaterial absorber based on a split-ring-cross resonator [J]. *Appl. Phys. A*, 2010, **102**(1): 99-103.
[7] Driessen E F C, Dood M J A d. The perfect absorber [J]. *Appl. Phys. Lett.*, 2009, **94**(17): 171109.
[8] Maier T, Brueckl H. Multispectral microbolometers for the midinfrared [J]. *Opt. Lett*, 2010, **35**(22): 3766-3768.
[9] Talghader J J, Gawarikar A S, Shea R P. Spectral selectivity in infrared thermal detection [J]. *Light: Science & Applications*, 2012, **1**(8): e24.
[10] Liu N, Mesch M, Weiss T, *et al.* Infrared perfect absorber and its application as plasmonic sensor [J]. *Nano Lett.*, 2010, **10**(7): 2342-2348.
[11] Landy N I, Sajuyigbe S, Mock J J, *et al.* Perfect Metamaterial Absorber [J]. *Phys. Rev. Lett.*, 2008, **100**(20): 207402.
[12] Zhu B, Wang Z B, Yu Z Z, *et al.* Planar metamaterial microwave absorber for all wave polarizations [J]. *Chin. Phys. Lett.*, 2009, **26**(11): 114102.
[13] Hu T, Landy N I, Bingham C M, *et al.* A metamaterial absorber for the terahertz regime: design, fabrication and characterization [J]. *Opt. Express*, 2008, **16**(10): 7181-7188.
[14] Watts C M, Liu X, Padilla W J. Metamaterial electromagnetic wave absorbers [J]. *Adv. Mater.*, 2012, 24(23): OP98-OP120.
[15] Wang J Q, Fan C Z, Ding P, *et al.* Tunable broad-band perfect absorber by exciting of multiple plasmon resonances at optical frequency [J]. *Opt. Express*, 2012, **20**(1): 14871-14878.
[16] Pu M B, Hu C G, Wang M, *et al.* Design principles for infrared wide-angle perfect absorber based on plasmonic structure [J]. *Opt. Express*, 2011, **19**(18): 17413-17420.
[17] Chen S Q, Cheng H, Yang H F, *et al.* Polarization insensitive and omnidirectional broadband near perfect planar metamaterial absorber in the near infrared regime [J]. *Appl. Phys. Lett.*, 2011, **99**(25): 253104.
[18] Liu X L, Tyler T, Starr T, *et al.* Taming the Blackbody with Infrared Metamaterials as Selective Thermal Emitters [J]. *Phys. Rev. Lett.*, 2011, **107**(4): 045901.
[19] Aydin K, Ferry V E, Briggs R M, *et al.* Broadband polarization-independent resonant light absorption using ultrathin plasmonic super absorbers [J]. *Nat. Commun.*, 2011, **2**: 517.
[20] Landy N I, Bingham C M, Tyler T, *et al.* Design, theory, and measurement of a polarization-insensitive absorber for terahertz imaging [J]. *Phys. Rev. B*, 2009, **79**(12): 125104.
[21] Hu T, Bingham C M, Strikwerda A C, *et al.* Highly flexible wide angle of incidence terahertz metamaterial absorber: Design, fabrication, and characterization [J]. *Phys. Rev. B*, 2008, **78**(24): 241103.
[22] Cheng H, Chen S Q, Yang H F, *et al.* A polarization insensitive and wide-angle dual-band nearly perfect absorber in the infrared regime [J]. *J. Opt.*, 2012, **14**(8): 085102.
[23] Hao J M, Wang J, Liu X L, *et al.* High performance optical absorber based on a plasmonic metamaterial [J]. *Appl. Phys. Lett.*, 2010, **96**(25): 251104.
[24] Wu C, Neuner B, Shvets G, *et al.* Large-area wide-angle spectrally selective plasmonic absorber [J]. *Phys. Rev. B*, 2011, **84**(7): 075102.
[25] Yamamoto K, Goericke F, Guedes A, *et al.* Pyroelectric aluminum nitride micro electromechanical systems infrared sensor with wavelength-selective infrared absorber [J]. *Appl. Phys. Lett.*, 2014, **104**(11): 111111.
[26] Bass M, LI G F, Stryland E V, *et al.* *Handbook of Optics* [M]. New York, USA: McGraw-Hill Professional, 2010.
[27] Palik E D. *Handbook of Optical Constants of Solids* [M]. USA: Academic Press, 1998.
[28] Dolling G, Wegener M, Soukoulis C M, *et al.* Negative-index metamaterial at 780 nm wavelength [J]. *Opt. Lett.*, 2007, **32**(1): 53-55.
[29] Dodge M J. Refractive properties of magnesium fluoride [J]. *Appl. Opt.*, 1984, **23**(12): 1980-1985.
[30] Dayal G, Ramakrishna S A. Design of highly absorbing metamaterials for infrared frequencies [J]. *Opt. Express*, 2012, **20**(16): 17503-17508.
[31] Lee H M, Wu J C. A wide-angle dual-band infrared perfect absorber based on metal-dielectric-metal split square-ring and square array [J]. *J. Phys. D: Appl. Phys.*, 2012, **45**(20): 205101.
[32] Zhu W R, Zhao X P, Gong B Y, *et al.* Optical metamaterial absorber based on leaf-shaped cells [J]. *Appl. Phys. A*, 2010, **102**(1): 147-151.
[33] Ye Y Q, Jin Y, He S. Omnidirectional, polarization-insensitive and broadband thin absorber in the terahertz regime [J]. *J. Opt. Soc. Am. B*, 2010, **27**(3): 498-504.